Granulometric analysis of condensed maltodextrin particles observed by scanning electron microscopy

Master MISPA

Ecole des Mines de Saint-Etienne – France

Student : Antoine BOTTENMULLER

Supervisors : Prof. Johan DEBAYLE & Prof. Yann GAVET

12/04/2023

Bibliography

- **[1]** D. Ioannou, W. Huda and A. F. Laine, “Circle recognition through a 2D Hough Transform and radius histogramming”, *Image and Vision Computing* 17 (1999), pp. 15-26
- **[2]** M. Smereka and I. Duleba, “Circular object detection using a modified Hough transform”, *International Journal of Applied Mathematics and Computer Science* 18 (2008), pp. 85-91
- **[3]** N. Guil and E. L. Zapata, “Lower order circle and ellipse Hough transform”, *Pattern Recognition*, Volume 30, No. 10 (1997), pp. 1729-1744
- **[4]** M. Mirzaei and H. K. Rafsanjani, “An automatic algorithm for determination of the nanoparticles from TEM images using circular Hough transform”, *Micron* 96 (2017), pp. 86-95
- **[5]** P. Muneesawang and C. Sirisathitkul, “Size measurement of nanoparticle assembly using multilevel segmented TEM images”, *Journal of Nanomaterials*, Volume 2015 (2015), 8 pages
- **[6]** J. Angulo and D. Jeulin, “Stochastic watershed segmentation”, International Symposium On Mathematical Morphology 8 (2007), pp. 256-276
- **[7]** F. Malmberg, C. L. Luengo Hendriks and R. Strand, “Exact evaluation of targeted stochastic watershed cuts”, *Discrete Applied Mathematics* 216 (2017), pp. 449-460

Bibliography

- **[8]** T. Zou, T. Pan, M. Taylor and H. Stern, "Recognition of overlapping elliptical objects in a binary image", *Pattern Analysis and Applications* 24 (2021), pp. 1193-1206
- **[9]** D. Jeulin, I. T. Villalobos and A. Dubus, "Morphological analysis of UO2 powder using a dead leaves model", *Microscopy Microanalysis Microstructures* 6 (1995), pp.371-384
- **[10]** C. Bordenave, Y. Gousseau and F. Roueff, "The dead leaves model : a general tessellation modelling occlusion", *Applied Probability Trust* 38 (2006), pp. 31-46
- **[11]** C. J. Gommes, "Stochastic models of disordered mesoporous materials for small-angle scattering analysis and more", *Microporous and Mesoporous Materials* 257 (2018), pp. 62-78
- **[12]** A. Ajdari Rad, K. Faez and N. Qaragozlou, "Fast circle detection using gradient pair vectors", Dicta (2003), 9 pages
- **[13]** T. J. Atherton and D.J. Kerbyson, "Size invariant circle detection", *Image and Vision Computing* 17 (1999), pp. 795-803
- **[14]** V. Ayala-Ramirez, C. H. Garcia-Capulin, A. Perez-Garcia and R. E. Sanchez-Yanez, "Circle detection on images using genetic algorithms", *Pattern Recognition Letters* (2006), pp. 652-657

Bibliography

- **[15]** A. Oualid Djekoune, K. Messaoudi and K. Amara, “Incremental circle Hough transform: an improved method for circle detection”, *Optik* 133 (2017), pp. 17-31
- **[16]** K. B. Bernander, K. Gustavsson, B. Selig, I-M. Sintorn and C. L. Luengo Hendriks, “Improving the stochastic watershed”, *Pattern Recognition Letters* 34 (2013), pp. 993-1000
- **[17]** N. Coudray, A. Dieterlen, L. Vidal, E. Roth, G. Trouvé and S. Bistac, “Image processing nanoparticles size measurement for determination of density values to correct the ELPI measures”, *Precision Engineering* 32 (2008), pp. 88-99
- **[18]** R. Cohn, I. Anderson, T. Prost, J. Tiarks, E. White and E. Holm, “Instance Segmentation for direct measurements of satellites in metal powders and automated microstructural characterization from image data”, *JOM* 73 (2021), pp. 2159-2172
- **[19]** M. Frei and F. E. Kruis, “Image-based size analysis of agglomerated and partially sintered particles via convolutional neural networks”, *Powder Technology* 360 (2020), pp. 324-336

Part 1

PROBLEM & CONTEXT

Problem and context

Problem of *image analysis* given by the ENSIACET (Toulouse INP) for the work of Daniel TOBON VELEZ

Topic : We have a set of greyscale SEM images of condensed maltodextrin particles

Problem : How to determine the particle size distribution in the given images?

=> Find and build an automatic method

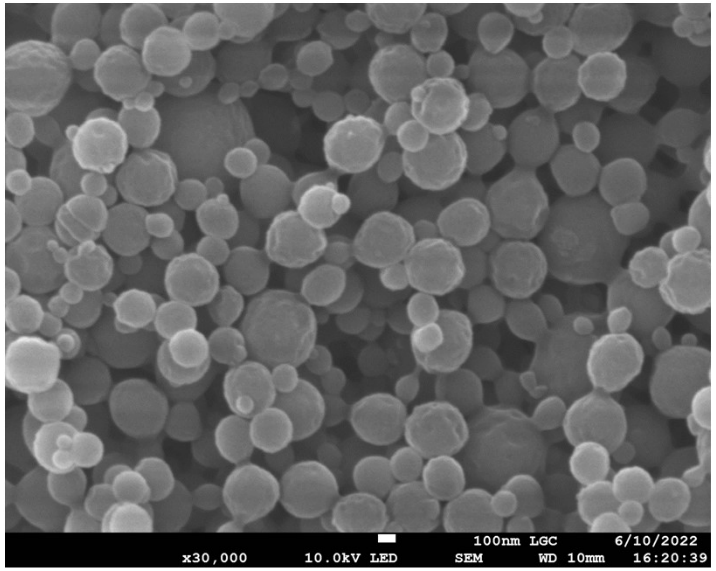

Figure 1 : Example of an image of grains to be analysed taken by Daniel TOBON VELEZ (zoom x30000) | Toulouse INP – ENSIACET

Problem and context

Data given : a set of 20 images (.bmp) representing condensed grains to analyse with different scales, and the respective descriptions (.txt files) of the taken SEM images' properties

More information given :

- we can consider all the grains as spherical, and so as disks on images
- the deepness of the grains doesn't influence their appearance's size
- the lightness isn't directly linked to the grain's position / deepness

Problem and context

a) b) c) d)

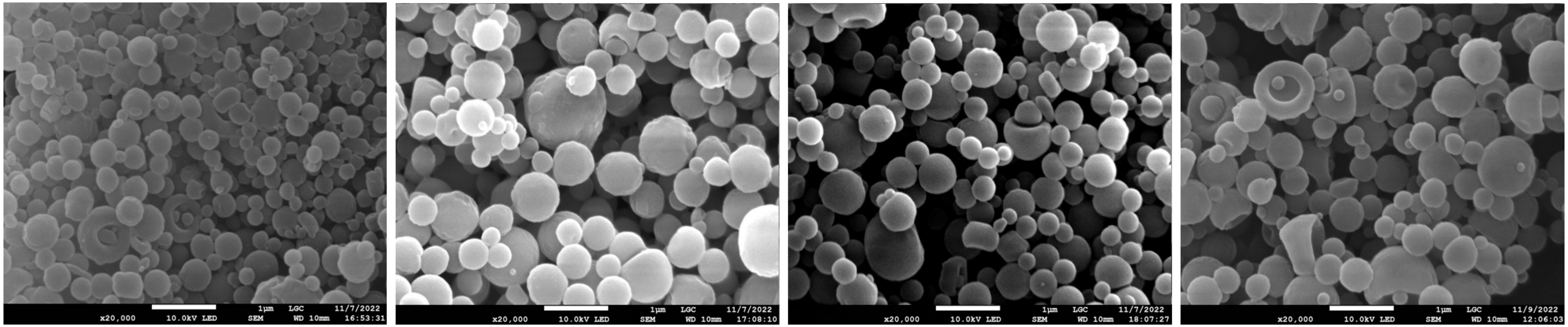

Figure 2 : Four examples of images given by the ENSIACET of the same grains sample with the same scale (zoom: x20,000).

4 main lines :

→ **Implementing** grains **segmentation methods**

→ **Developing** a stochastic **grains simulation model**

→ **Comparing** methods' **accuracy** on **simulated images**

→ **Applying** the methods on **real images**

Part 2

SEGMENTATION METHODS

Segmentation methods

From the literature

- ***Stochastic Watershed* (SW)**:

Enhances the results by accumulating multiple watershed realizations with random markers. A distance transform is applied on the binarized extracted contours. The local maxima are calculated and defined as the centres of the different circles on the map, and the value of the distance gives their radius.

- ***Circular Hough Transform* (CHT)**:

After a low-pass filter on the gradient magnitude image and a binarization of the contours, a discrete three-dimensional CHT space is built and the circles are extracted from the local maxima in the space.

Segmentation methods

Problem: Either **under** or **over**-segmentation!

a) b) c)

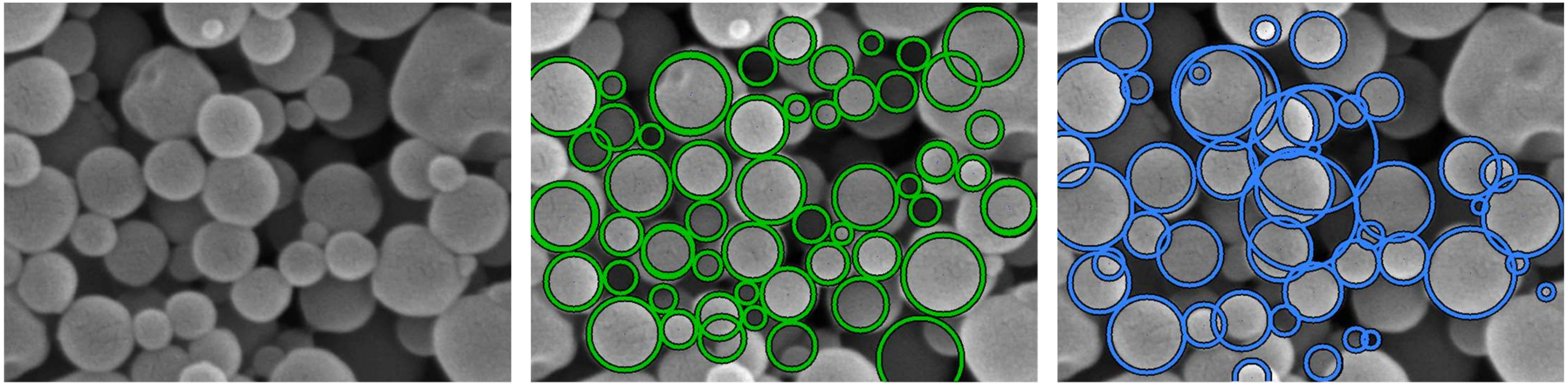

Figure 3 : Example of the application of the two segmentation methods to a real image. From left to right: Original image (a), results of the segmentation with the Stochastic Watershed (b), and results with the circular Hough transform (c).

Proposed: Curvature Analysis Method (CAM)

Main principle:

A procedural algorithm based on the analysis of the curvature of the thin arcs of the grains' contours.

3 main steps :

- Building of the linear minimum MSE map
- Extraction of the thin arcs of the grains' contours
- Circles association and rearrangement

MINES Saint-Étienne

Step 1: Building of the linear minimum MSE map

Objective: Associating to each pixel the minimum value of the error function E_{p_c} from the gradient magnitude image ∇, where E_{p_c} is defined in a window as follows:

$$E_{p_c}(\alpha) = \frac{1}{\sum_{i=1}^{n} \nabla(p_i)} \sum_{i=1}^{n} d\left(p_i, L_{p_c,\alpha}\right)^2 \nabla(p_i)$$

With : $(p_i)_{i \in [\![1,n]\!]}$ the family of n points in the window centred to p_c ;
$L_{p_c,\alpha}$ the line of slope α crossing p_c in the image's coordinates ;
$d\left(p_i, L_{p_c,\alpha}\right)$ the Euclidean distance between p_i and $L_{p_c,\alpha}$.

Step 1: Building of the linear minimum MSE map

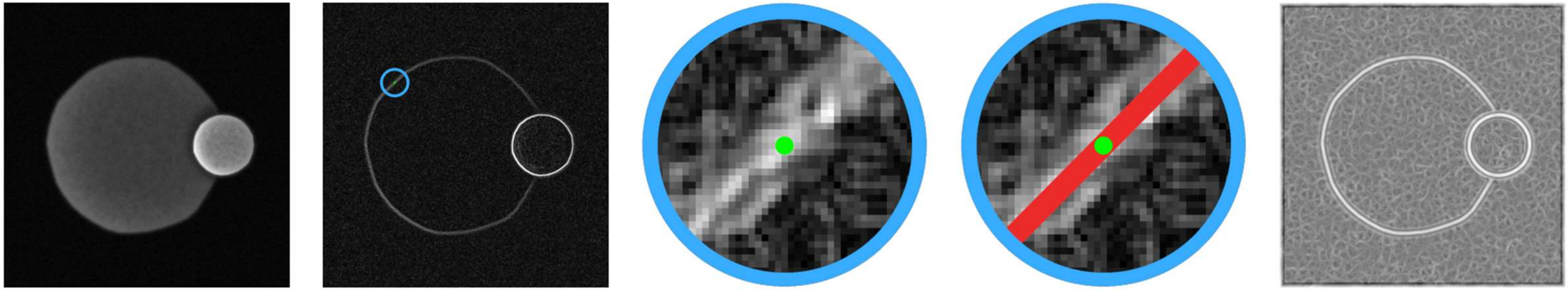

(a) Original image. (b) Gradient magnitude with the circular window (blue) centred on a pixel p_c. (c) View on the one window with the centre p_c (green). (d) Line $L_{p_c,\alpha}$ (red) going by p_c and minimizing the weighted MSE function. (e) Linear minimum MSE map.

Figure 4 : Construction steps of the linear minimum MSE map.

Segmentation methods

Step 2: Extraction of the thin arcs of the grains' contours

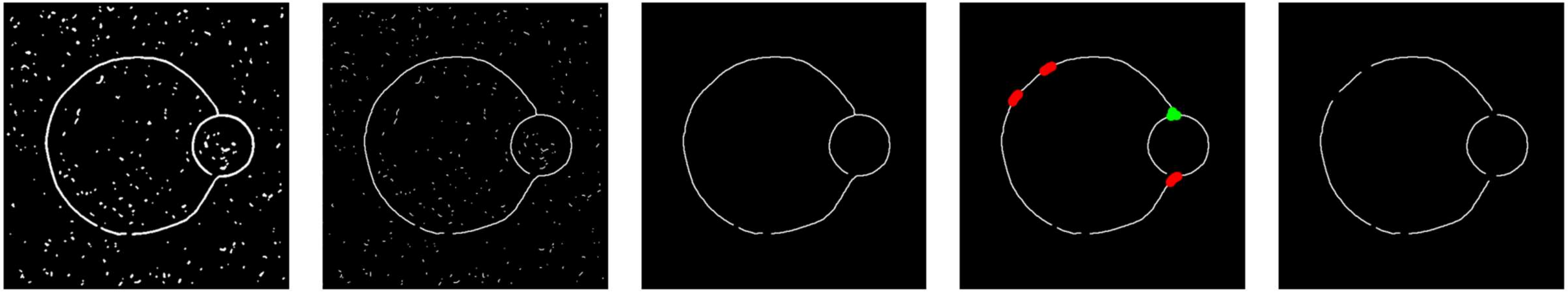

(a) Binarized image of the linear minimum MSE map from Fig. 2e.

(b) Binary image skeleton.

(c) Clean skeleton.

(d) Intersection area (green) and curvature irregularities (red) on clean skeleton.

(e) Final split arcs.

Figure 5 : Steps of the extraction of the thin arcs.

Segmentation methods

Step 3: Circles association and rearrangement

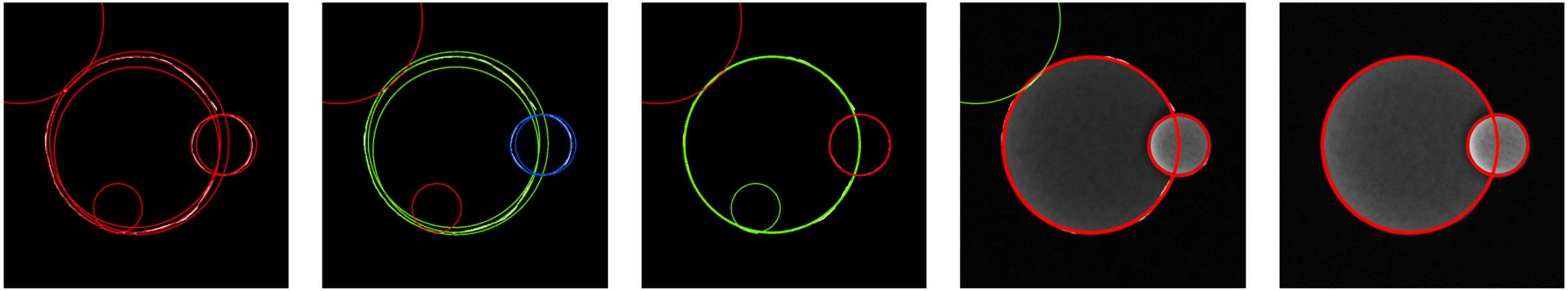

(a) All circles from arcs with an error below a threshold.

(b) Circles close enough in the space (x_p, y_p, r) to be merged, green and blue being two clusters of merging circles.

(c) Circles sharing arcs close enough from the circles edges to be merged, green being one cluster of two merging circles.

(d) Circles being brighter inside their arc than outside (green) are removed.

(e) Final detected circles.

Figure 6 : Steps of circles association and rearrangement.

Application to a real image (example)

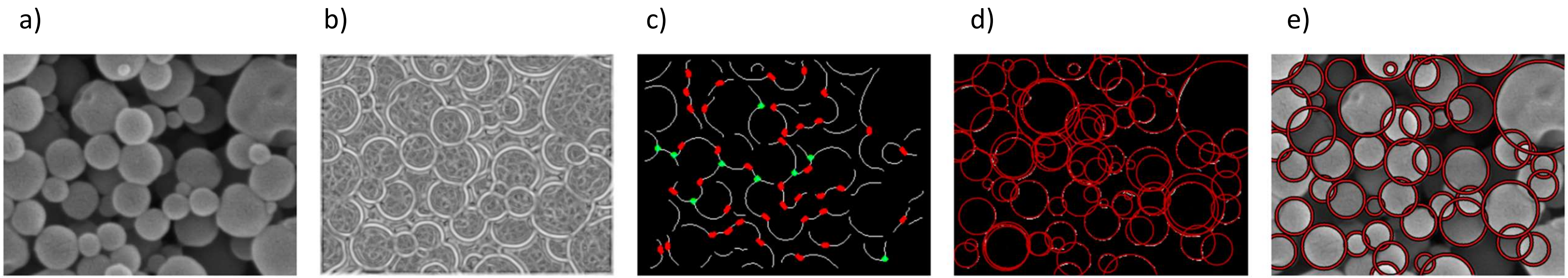

Figure 7 : Application of the CAM on a real image. From left to right: Original image (Fig. 6a), normalized linear minimum MSE map (Fig. 6b), clean skeleton from the binarized minimum MSE map, with detected intersections (green) and curvature splits (red) (Fig. 6c), computed circles for all arcs from the skeleton (Fig. 6d), and final circles segmentation (Fig. 6e).

Part 3

STOCHASTIC GRAINS SIMULATION MODEL

Simulation model

Objectives of the model:

Generate **random and realistic images** of condensed grains like the real ones, for which the **ground truth is known**.

Use the generated images to **validate the new segmentation method** (CAM) by comparing its **accuracy** to the two others' one (SW and CHT).

Generation:

The model generates **random grains** and add them randomly on a black image **one after the other**.

Figure 8 : Example of the generation of a grain. From left to right: Binary shape of the grain (a), lighting effects added to the shape regarding le light source's position (b), and the shadow associated to the shape (c).

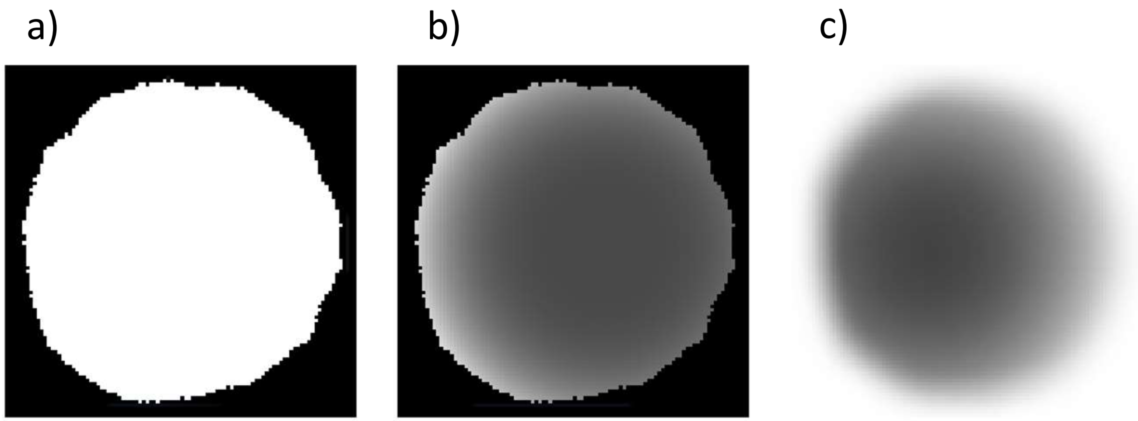

Example of a generated image:

Figure 9 : Example of a generated image. After all the grains are added to the black image, the image is **blurred** at different depth layers and **Gaussian noise** is added.

Random law on grains radii:

bimodal =

{ [35, 10] (**0.8**) ,
[60, 14] (**0.2**)

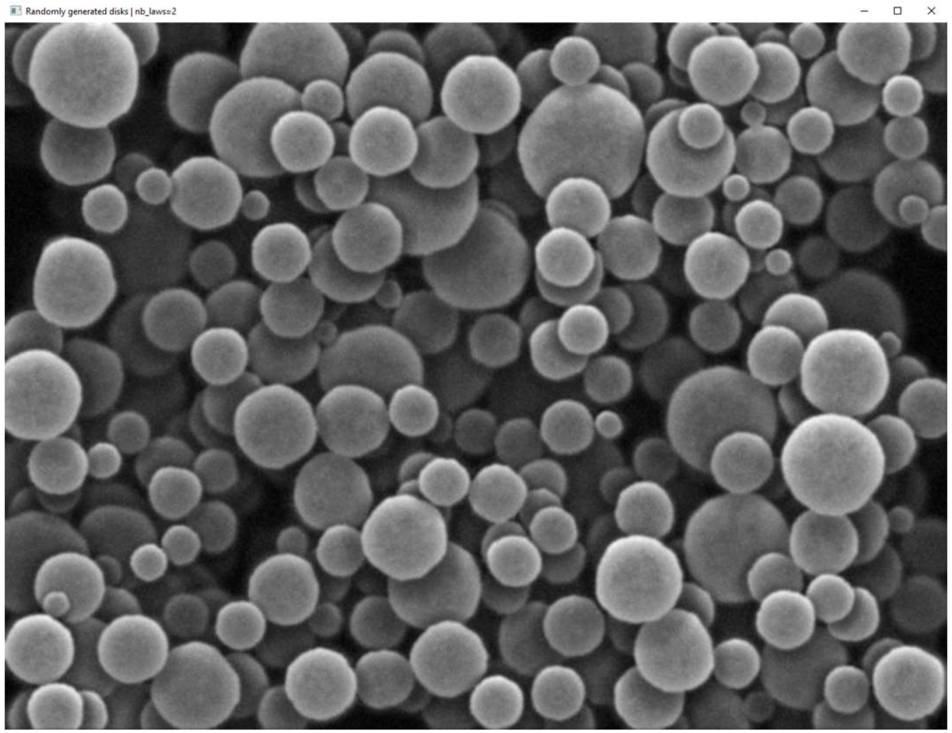

Simulation model

Variables subjected to random :

- Number of particles (200 +/- 50 [uniform])
- Sizes of particles (law can be defined. Here: bimodal)
- Position of particles (uniform law on maxima of distance map)
- Light source orientation (uniform law on angles: see folder)
- Appearance of each grain (uniform law on gradient of edges)

Little physics properties added to get more realistic :
collision between grains

Part 4

APPLICATION TO SIMULATED IMAGES

Visual comparison: Application of the three methods on an image

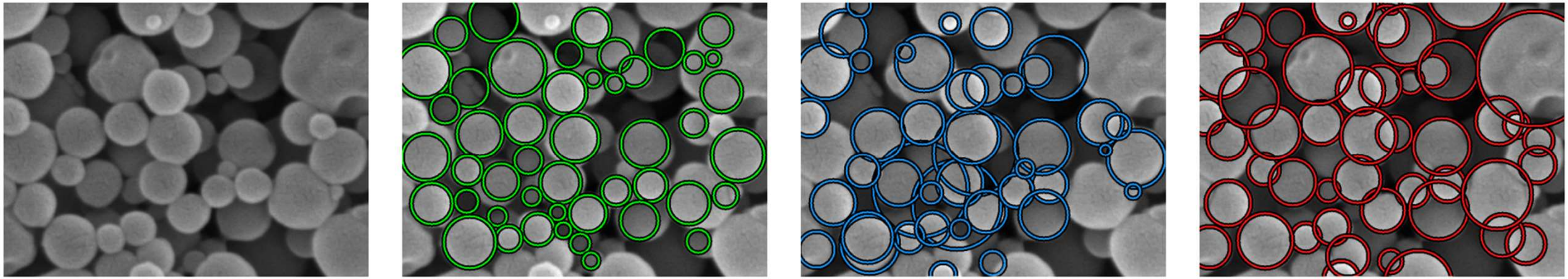
(a) Original image. (b) Segmentation with SW ($N = 40$). (c) Segmentation with CHT. (d) Segmentation with CAM.

Figure 10 : Example of results from the three segmentation methods on real image with the best inner-parameters set.

On simulated images

100 simulated images have been generated with two random laws on the grains’ radii :

- A bimodal law (100 images)
- A log-normal law (100 images)

The three segmentation methods (SW, CHT and CAM) have been applied on them, and their Particle Size Distribution (PSD) has been built for the two laws and compared to the ground truth.

Results (PSD)

Figure 11 : Resulting PSDs on the bimodal law (top) and the log-normal law (bottom), expressed in number (left) and in volume (right).

Green : SW

Blue : CHT

Red : CAM

Dotted black : ground truth

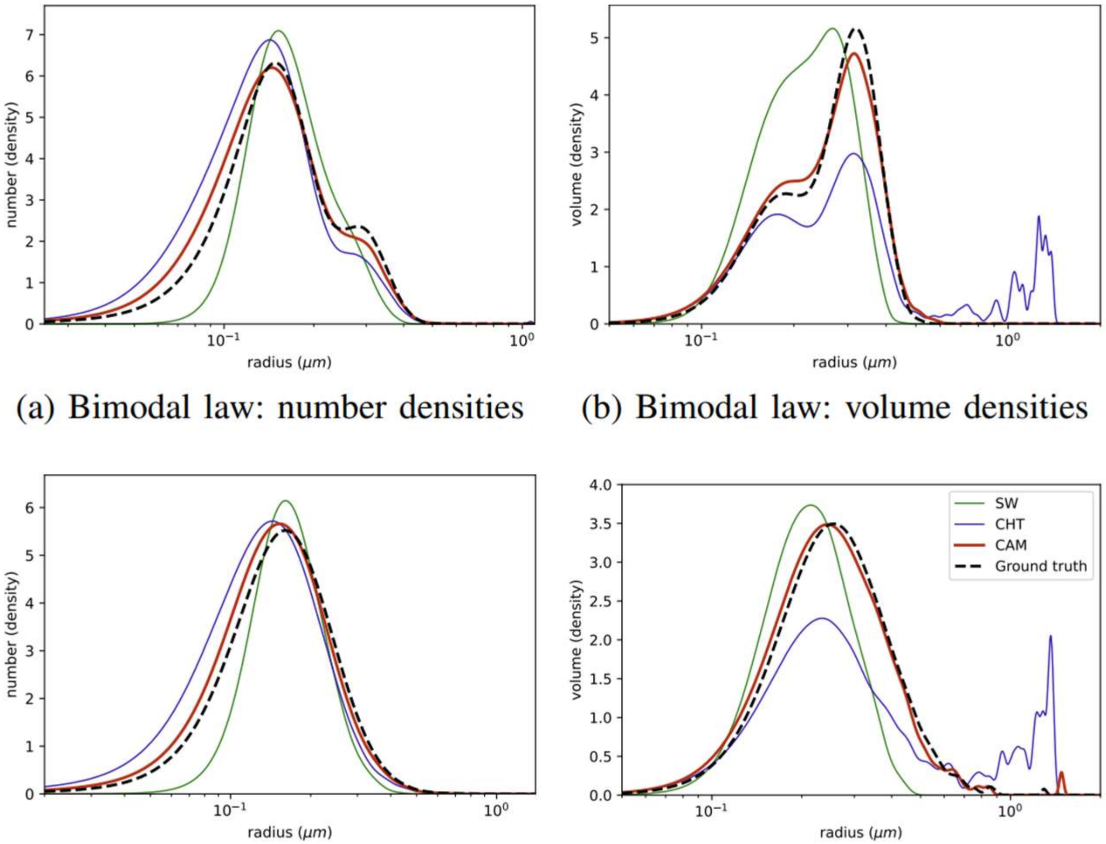

(a) Bimodal law: number densities (b) Bimodal law: volume densities

(c) Log-normal law: number densities (d) Log-normal law: volume densities

Results (mean & STD)

Properties	Ground truth	SW	CHT	CAM
Mean	0.199 μm	0.190 μm	0.180 μm	0.191 μm
STD	0.082 μm	0.058 μm	0.101 μm	0.082 μm

TABLE I: Mean and STD of densities on bimodal law.

Properties	Ground truth	SW	CHT	CAM
Mean	0.199 μm	0.187 μm	0.182 μm	0.190 μm
STD	0.082 μm	0.054 μm	0.104 μm	0.081 μm

TABLE II: Mean and STD of densities on log-normal law.

Observation

SW: is concentrated around its mean (no extreme radius values)

CHT: too many extreme values (too many false little and large circles)

CAM: seems to be the closed one to the ground truth
seems to be well balanced (number & values)

Part 5

RESULTS ON REAL IMAGES…

Results on real images

The three segmentation methods are applied to **20 real given images**.

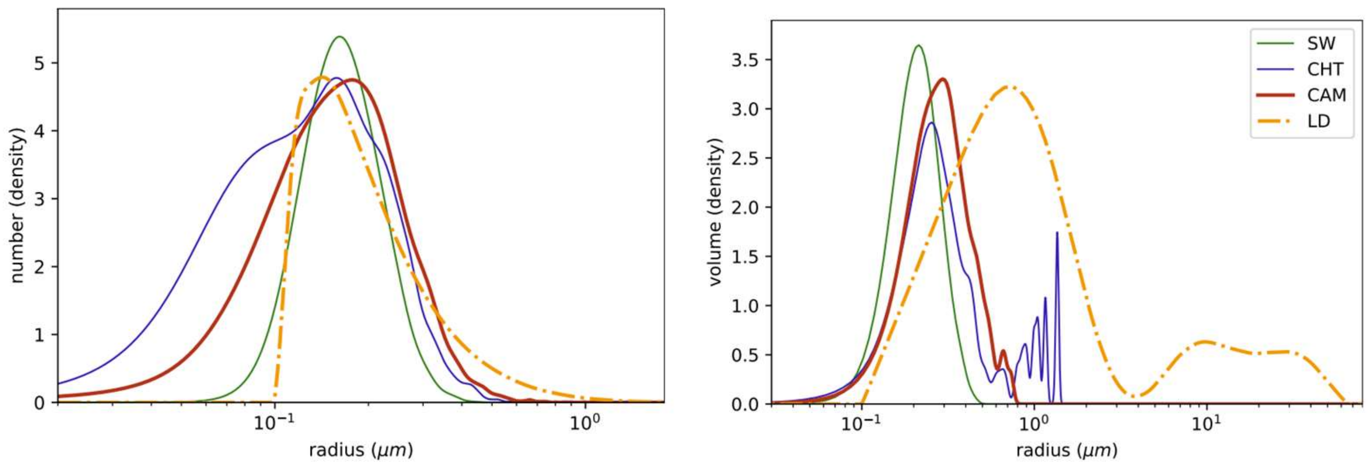

(a) Real images: number densities (b) Real images: volume densities

Figure 12 : Diagrams of densities (PSD) on real images
– Comparison to Laser Diffraction (LD), yellow

MINES Saint-Étienne

Results (mean & STD)

Properties	LD	SW	CHT	CAM
Mean	0.217 μm	0.185 μm	0.184 μm	0.207 μm
STD	0.133 μm	0.052 μm	0.105 μm	0.093 μm

TABLE III: Mean and STD of densities on real images.

MINES Saint-Étienne

Observation

SW: is still concentrated around its mean (no extreme radius values)

CHT: still too many extreme values (too many little and large circles)

CAM: still seems to be well balanced (number & values)

As the CAM can be considered giving a good estimation of the true density of the PSD, the results from the LD cannot be considered as trustworthy.

Part 6

CONCLUSION

Conclusion

✓ In simulations, the CAM is more accurate than the SW and than the CHT in both PSD in number and PSD in volume.

✓ Based on the results given by the CAM, the grains from real images can be considered as following a log-normal law with a mean of 0.207 µm and a standard deviation of 0.093 µm.

✓ The laser diffraction can not be considered as a trustworthy granulometric tool as its PSDs are far from observation.

For a future work: try deep learning methods and compare the results to the ones obtained in this study

Thank you
for your attention!

Questions / Comments

Student : Antoine BOTTENMULLER

Supervisors : Prof. Johan DEBAYLE & Prof. Yann GAVET

12/04/2023